Many-Body Quantum Dynamics by the Reduced Density Matrix Based on Time-Dependent Density-Functional Theory

Vladimir U. Nazarov*
Research Center for Applied Sciences, Academia Sinica, Taipei 11529, Taiwan

(Received 8 April 2019; published 29 August 2019)

We evaluate the density matrix of an arbitrary quantum mechanical system in terms of the quantities pertinent to the solution of the time-dependent density functional theory (TDDFT) problem. Our theory utilizes the adiabatic connection perturbation method of Görling and Levy, from which the expansion of the many-body density matrix in powers of the coupling constant λ naturally arises. We then find the reduced density matrix $\rho_\lambda(\mathbf{r},\mathbf{r}',t)$, which, by construction, has the λ independent diagonal elements $\rho_\lambda(\mathbf{r},\mathbf{r},t)=n(\mathbf{r},t)$, $n(\mathbf{r},t)$ being the particle density. The off-diagonal elements of $\rho_\lambda(\mathbf{r},\mathbf{r}',t)$ contribute importantly to the processes unaccessible via the density, directly or by the use of the known TDDFT functionals. Of those, we consider the momentum-resolved photoemission, doing this to the first order in λ, i.e., on the level of the exact exchange theory. In illustrative calculations of photoemission from the quasi-2D electron gas and isolated atoms, we find quantitatively strong and conceptually far-reaching differences with the independent-particle Fermi's golden rule formula.

DOI: 10.1103/PhysRevLett.123.095302

Time-dependent (TD) density functional theory (TDDFT) [1–3] is a widely used powerful method to study the time-evolution and the excitation processes in quantum mechanical systems. Its success is due to the crucial simplification arising from the substitution of the prohibitively complicated many-body problem with the reference single-particle one, keeping (apart from approximations possibly invoked) the exact TD electron density of the original many-body system. The description of a number of physical processes (e.g., optical absorption [4,5], slowing of ions in matter [6,7], impurity resistivity of metals [8], etc.) can be rigorously reduced to finding the TD electron density, making TDDFT the method of choice for studying those classes of phenomena.

There exist, at the same time, fundamental processes and the corresponding experimental methods, the theory of which cannot, on the very general physical grounds, be formulated explicitly in terms of the particle density. For a clear example, the momentum-resolved photoemission requires the knowledge of the probability in the momentum space, which, as long as we remain within the framework of the consistent quantum mechanics, cannot be found directly from the probability in the coordinate space, the latter giving the particle density. The necessary information is, in this case, contained in the reduced density matrix (DM) ρ [9]. The real space $\rho(\mathbf{r},\mathbf{r}',t)$ and the momentum space $\rho(\mathbf{p},\mathbf{p}',t)$ representations of ρ are related by the double Fourier transform, while the diagonal elements in the corresponding representations (probabilities) cannot be related directly [10].

To find the reduced DM is a complicated problem, generally speaking, taking us back to the many-body theory. In this Letter we come up with the observation that the solution of this task can be greatly facilitated if the TDDFT problem for the same system has been already solved. We use the power of the adiabatic connection perturbation method [11,12] and show that, changing the electron-electron (e-e) interaction constant λ continuously from zero (for the reference system) to one (for the physical system), while keeping the particle density $n_\lambda(\mathbf{r})=n(\mathbf{r})$ unchanged, we determine not only the Kohn-Sham (KS) [13] potential $v_s(\mathbf{r},t;\lambda)$, but also the many-body DM $\hat\rho_\lambda$. The latter can be readily reduced to the one-DM $\rho_\lambda(\mathbf{r},\mathbf{r}',t)$ expressed through the KS TDDFT quantities. We emphasize, and this is the motivation of this work, that $\rho_{\lambda=1}(\mathbf{r},\mathbf{r}',t)$ is, while the KS DM is not, the true reduced DM of the physical system (cf., Ref. [14]).

Practically, the above program can so far be implemented to the first order in λ only, which results in the construction of the TD exact-exchange (TDEXX)-based theory of the DM. We apply this theory to the problem of the momentum-resolved photoemission, finding quantitative and qualitative differences with Fermi's golden rule. We use atomic units ($e^2=m_e=\hbar=1$).

Real-time formalism for DM to the first order in the interaction.—We write the adiabatic connection Hamiltonian for an N-particle system [11,12]

$$\hat H(t;\lambda)=\sum_{i=1}^{N}\left[-\frac{1}{2}\Delta_i+v_{\rm ext}(\mathbf{r}_i,t)+\tilde v(\mathbf{r}_i,t;\lambda)\right]+\sum_{i<j}^{N}\frac{\lambda}{|\mathbf{r}_i-\mathbf{r}_j|},\qquad(1)$$

where $\lambda \in [0,1]$, $\tilde{v}(\mathbf{r},t;0) = v_s(\mathbf{r},t) - v_{\mathrm{ext}}(\mathbf{r},t)$, v_{ext} and v_s being the external and KS potentials, respectively, and we keep the particle density λ independent. The corresponding N-body DM obeys Liouville's equation

$$i\frac{\partial \hat{\rho}(t;\lambda)}{\partial t} = [\hat{H}(t;\lambda), \hat{\rho}(t;\lambda)]. \tag{2}$$

Expanding to the first order in λ (but making, so far, no assumption regarding the strength of the external TD field), we write

$$\begin{bmatrix} \hat{H}(t;\lambda) \\ \hat{\rho}(t;\lambda) \\ \tilde{v}(t;\lambda) \end{bmatrix} = \begin{bmatrix} \hat{H}_0(t) \\ \hat{\rho}_0(t) \\ \tilde{v}_0(t) \end{bmatrix} + \lambda \begin{bmatrix} \hat{H}_1(t) \\ \hat{\rho}_1(t) \\ \tilde{v}_1(t) \end{bmatrix}, \tag{3}$$

where

$$\hat{H}_0(t) = \sum_{i=1}^{N} \left[-\frac{1}{2}\Delta_i + v_{\mathrm{ext}}(\mathbf{r}_i,t) + \tilde{v}_0(\mathbf{r}_i,t) \right], \tag{4}$$

$$\hat{H}_1(t) = \sum_{i=1}^{N} \tilde{v}_1(\mathbf{r}_i,t) + \sum_{i<j}^{N} \frac{1}{|\mathbf{r}_i - \mathbf{r}_j|}, \tag{5}$$

and the corresponding density matrices evolve as

$$i\frac{\partial \hat{\rho}_0(t)}{\partial t} = [\hat{H}_0(t), \hat{\rho}_0(t)], \tag{6}$$

$$i\frac{\partial \hat{\rho}_1(t)}{\partial t} = [\hat{H}_0(t), \hat{\rho}_1(t)] + [\hat{H}_1(t), \hat{\rho}_0(t)]. \tag{7}$$

Let for $t \leq 0$ the system be in its ground state with the KS wave function $|0\rangle$, where $|\alpha\rangle$ is the orthonormal complete set of the Slater-determinant eigenfunctions of $\hat{H}_0(0)$. Let at $t = 0$ the TD potential be switched on. Then, since $\hat{H}_0(t)$ is self-conjugate, $|\alpha(t)\rangle$, which satisfy

$$i\frac{\partial |\alpha(t)\rangle}{\partial t} = \hat{H}_0(t)|\alpha(t)\rangle, |\alpha(0)\rangle = |\alpha\rangle, \tag{8}$$

constitute also an orthonormal complete set at each t. From Eqs. (6) and (7) we obtain (Supplemental Material [15], Sec. I)

$$\langle \alpha(t)|\hat{\rho}_0(t)|\beta(t)\rangle = \delta_{\alpha 0}\delta_{\beta 0}, \tag{9}$$

$$\langle \alpha(t)|\hat{\rho}_1(t)|\beta(t)\rangle = i(\delta_{\alpha 0} - \delta_{\beta 0}) \int_{-\infty}^{t} \langle \alpha(t')|\hat{H}_1(t')|\beta(t')\rangle dt', \tag{10}$$

where $\delta_{\alpha\beta}$ is the Kronecker symbol. Transforming Eqs. (9) and (10) to real space and reducing to the one DM, we find

$$\rho_0(\mathbf{r},\mathbf{r}',t) = \sum_{i\in \mathrm{occ}} \phi_i(\mathbf{r},t)\phi_i^*(\mathbf{r}',t), \tag{11}$$

$$\begin{aligned} \rho_1(\mathbf{r},\mathbf{r}',t) = &\sum_{\substack{i\in \mathrm{occ} \\ j \in \mathrm{unocc}}} \langle 0(t)|\hat{\rho}_1(t)|0_{ij}(t)\rangle \phi_i(\mathbf{r},t)\phi_j^*(\mathbf{r}',t) \\ &+ (\mathbf{r} \leftrightarrow \mathbf{r}')^*, \end{aligned} \tag{12}$$

where ϕ_i are KS orbitals, $0_{ij}(t)$ is the propagated ground-state Slater-determinant $0(t)$ with the ith orbital replaced with the jth one [the matrix elements in Eq. (12) are the only ones surviving the integration]. Equation (12) reduces to

$$\begin{aligned} &\rho_1(\mathbf{r},\mathbf{r}',t) \\ &\quad = -i \sum_{\substack{i\in \mathrm{occ} \\ j \in \mathrm{unocc}}} \int_{-\infty}^{t} dt' \bigg(\int v_x(\mathbf{r}_1,t')\phi_i^*(\mathbf{r}_1,t')\phi_j(\mathbf{r}_1,t') d\mathbf{r}_1 \\ &\qquad + \int \frac{\phi_i^*(\mathbf{r}_1,t')\rho_0(\mathbf{r}_1,\mathbf{r}_2,t')\phi_j(\mathbf{r}_2,t')}{|\mathbf{r}_1 - \mathbf{r}_2|} d\mathbf{r}_1 d\mathbf{r}_2 \bigg) \\ &\qquad \times \phi_i(\mathbf{r},t)\phi_j^*(\mathbf{r}',t) + (\mathbf{r} \leftrightarrow \mathbf{r}')^*, \end{aligned} \tag{13}$$

where $v_x = v_s - v_{\mathrm{ext}} - v_H$, and v_H are the exchange and the Hartree potentials, respectively.

Setting $\mathbf{r}' = \mathbf{r}$ in Eq. (13) and equating to zero (the density must be λ independent), we retrieve the TD version of the optimized effective potential equation [16–18] for $v_x(\mathbf{r},t)$. On the other hand, if above we allowed for nonmultiplicative effective potentials, then Eq. (13) would reproduce the long-known result [19] that the Hartree-Fock (HF) potential nullifies $\rho_1(\mathbf{r},\mathbf{r}',t)$. Consequently, the (TD) HF reduced DM is the first-order approximation to the physical one. As discussed above, this is not the case with TDDFT.

It is verifiable by the direct substitution that ρ_0 of Eq. (11) and ρ_1 of Eq. (13) satisfy the Liouville-type equations

$$i\frac{\partial \rho_0(\mathbf{r},\mathbf{r}',t)}{\partial t} = [\hat{h}_s(t), \rho_0(t)], \tag{14}$$

$$\begin{aligned} i\frac{\partial \rho_1(\mathbf{r},\mathbf{r}',t)}{\partial t} = &[\hat{h}_s(t), \rho_1(t)] - [v_x(t), \rho_0(t)] \\ &+ \int \rho_0(\mathbf{r},\mathbf{r}_1,t)\rho_0(\mathbf{r}_1,\mathbf{r}',t) \\ &\times \left[\frac{1}{|\mathbf{r}_1 - \mathbf{r}'|} - \frac{1}{|\mathbf{r}_1 - \mathbf{r}|} \right] d\mathbf{r}_1, \end{aligned} \tag{15}$$

where $\hat{h}_s(t)$ is the KS Hamiltonian. Equation (13) or, alternatively, Eq. (15) determine the time evolution of the reduced DM to the first order in the interaction, and they are expected to be useful in the nonlinear dynamics. We, however, turn now to the linear response regime and focus on the photoemission spectroscopy (PES) application.

Linear-response theory.—From now on we assume the TD external potential

$$v_{\text{ext}}^{(1)}(\mathbf{r},t)=\frac{1}{2}[v_{\text{ext}}^{(1)}(\mathbf{r},\omega)e^{-i\omega t}+\text{c.c.}] \tag{16}$$

to be weak. We expand $\rho(t)=\rho^{(0)}+\rho^{(1)}(t)+\rho^{(2)}(t)+\cdots$, where the superscripts stand for the orders in the strength of the TD perturbation, while the subscripts remain reserved for the orders in the *e*-*e* interaction. To the zeroth order in the latter, we obtain for the probability per unit time for an electron to be emitted into the state $\phi_f(\mathbf{r})$ (Supplemental Material [15], Sec. II) [20],

$$\lim_{t\to\infty}\frac{\langle\phi_f|\rho_0^{(2)}(t)|\phi_f\rangle}{t}=\sum_{i\in\text{occ}}A_{fi}(\omega)\delta(\omega-\epsilon_f+\epsilon_i), \tag{17}$$

where

$$A_{fi}(\omega)=\frac{\pi}{2}|\langle\phi_f|v_s^{(1)}(\omega)|\phi_i\rangle|^2, \tag{18}$$

reproducing the conventional Fermi's golden rule. To the *first* order in the interaction, Eq. (15) leads to (Supplemental Material [15], Sec. III)

$$\lim_{t\to\infty}\frac{\langle\phi_f|\rho_1^{(2)}(t)|\phi_f\rangle}{t}=\sum_{i\in\text{occ}}\Delta A_{fi}(\omega)\delta(\omega-\epsilon_f+\epsilon_i)+\Delta B_{fi}(\omega)\delta'(\omega-\epsilon_f+\epsilon_i), \tag{19}$$

$$\begin{aligned}\Delta A_{fi}(\omega)=-\pi\text{Re}\Bigg\{\langle\phi_f|v_s^{(1)}(\omega)|\phi_i\rangle^*\Bigg[&\langle\phi_f|v_x^{(1)}(\omega)|\phi_i\rangle+\sum_{k\neq i}C_{ki}\frac{\langle\phi_f|v_s^{(1)}(\omega)|\phi_k\rangle}{\epsilon_i-\epsilon_k}\\&+\sum_{k\neq f}C_{fk}\frac{\langle\phi_k|v_s^{(1)}(\omega)|\phi_i\rangle}{\epsilon_f-\epsilon_k}+\sum_{kl}(f_k-f_l)\frac{\langle\phi_k|v_s^{(1)}(\omega)|\phi_l\rangle}{\epsilon_k-\epsilon_l-\omega-i\eta}\int\frac{\phi_i(\mathbf{r})\phi_f^*(\mathbf{r}')\phi_l^*(\mathbf{r})\phi_k(\mathbf{r}')}{|\mathbf{r}-\mathbf{r}'|}d\mathbf{r}d\mathbf{r}'\Bigg]\Bigg\},\end{aligned} \tag{20}$$

$$\Delta B_{fi}(\omega)=-\frac{\pi}{2}|\langle\phi_f|v_s^{(1)}(\omega)|\phi_i\rangle|^2C_{ii}, \tag{21}$$

$$C_{km}=\langle\phi_k|v_x^{(0)}|\phi_m\rangle+\int\rho_0^{(0)}(\mathbf{r},\mathbf{r}')\frac{\phi_k^*(\mathbf{r})\phi_m(\mathbf{r}')}{|\mathbf{r}-\mathbf{r}'|}d\mathbf{r}d\mathbf{r}', \tag{22}$$

f_k being the orbitals' occupancies. Equations (19)–(22) generalize Fermi's golden rule by including interaction to the first order.

The two terms in Eq. (19) have distinct physical meaning: The one with the delta function accounts for the change in the *amplitude* of the emission due to the *e*-*e* interaction. The one with the delta-function derivative accounts for the excitation energies shifts, due to the same reason. To demonstrate this, we combine Eqs. (17) and (19) as

$$\begin{aligned}\lim_{t\to\infty}&\frac{\langle\phi_f|\rho^{(2)}(t)|\phi_f\rangle}{t}\\&=\sum_{i\in\text{occ}}[A_{fi}(\omega)+\Delta A_{fi}(\omega)]\delta(\omega-\epsilon_f+\epsilon_i)\\&\quad+\Delta B_{fi}(\omega)\delta'(\omega-\epsilon_f+\epsilon_i)\\&=\sum_{i\in\text{occ}}[A_{fi}(\omega)+\Delta A_{fi}(\omega)]\delta[\omega-\epsilon_f+\epsilon_i+\Delta\omega_i],\end{aligned} \tag{23}$$

where

$$\Delta\omega_i=\frac{\Delta B_{fi}(\omega)}{A_{fi}(\omega)}=-C_{ii}. \tag{24}$$

Importantly, the energy-shift [Eq. (24)] is a ground-state property of the KS system. We now turn to illustrative calculations.

Photoemission from quasi-2D electron gas with one filled subband.—For quasi-2D electron gas (Q2DEG) with one filled subband and normally applied electric field (schematized in Fig. 1) the analytical solution to the TDEXX problem exists [21], which makes it ideally suited for the illustration of our theory by a simple calculation. Then

$$v_x(z,t)=-\frac{1}{n_s}\int\frac{F_2(k_F|z-z'|)}{|z-z'|}n(z',t)dz', \tag{25}$$

where $F_2(u)=1+[L_1(2u)-I_1(2u)]/u$, L_1 and I_1 are the 1st-order modified Struve and Bessel functions, $n_s=\int_{-\infty}^{\infty}n(z,t)dz$ is the time-independent 2D density, and k_F is the corresponding 2D Fermi radius. From Eqs. (18), (20)–(21), we find $A_{f0}(\omega)$, $\Delta A_{f0}(\omega)$, and $\Delta\omega$ (Supplemental Material [15], Sec. IV). In particular,

$$\Delta\omega(k_{\|})=-\int|\mu_0(z)|^2G_{k_{\|}}(z)dz, \tag{26}$$

where $\mathbf{k}_{\|}$ is the conserving in-plane momentum,

$$G_{k_{\|}}(z)=v_x^{(0)}(z)+k_F\int|\mu_0(z')|^2S_{k_{\|}}(k_F|z-z'|)dz', \tag{27}$$

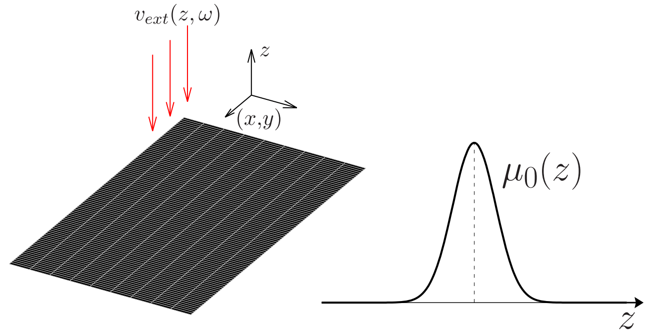

FIG. 1. Left: Schematics of the Q2DEG with one filled subband. Right: Schematics of the wave function of the only filled subband.

$$S_{k_\parallel}(u) = \int_0^\infty \frac{J_1(x)J_0(\frac{k_\parallel}{k_F}x)}{\sqrt{x^2+u^2}}dx, \tag{28}$$

and $J_n(x)$ are Bessel functions [see Ref. [15], Sec. IV for the plot of $S_{k_\parallel}(u)$].

In Fig. 2 we plot the ionization potential (IP). The IP with the interactions included (the solid curve for the EXX calculation) depends on $k_\parallel$. This dependence signifies a fundamental difference between the KS and the many-body dynamics: Our system is uniform in the xy plane and, therefore, xy and z coordinates separate in the KS equations, resulting in the motion of a KS electron in the z dimension being unaffected by the value of its in-plane momentum. In particular, the IP in the KS dynamics is $k_\parallel$ independent (shown with horizontal lines). Secondly, depending on $k_\parallel$, the energy shift can be either positive or negative. Therefore, for larger $k_\parallel$, we can emit an electron with the photon energy ω less than the KS work function $-\epsilon_0$. We stress that these results are not in contradiction to the theorem stating that the minus highest occupied KS orbital energy is IP [22] (IP-theorem), since the latter has been proven for finite number of particles (and then $k_\parallel$ is not defined), while here the number of particles is infinite [23].

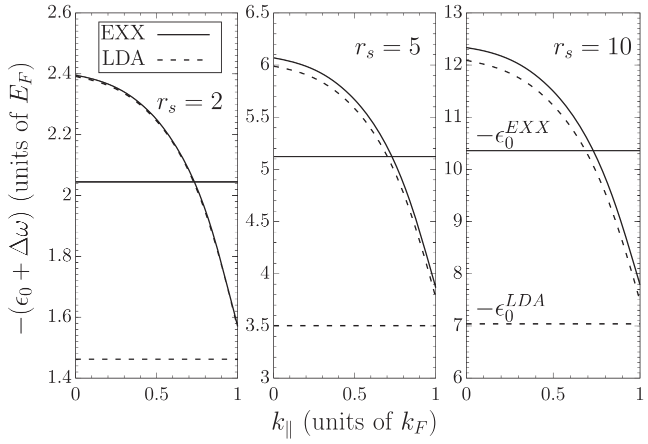

FIG. 2. IP obtained with the use of Eq. (26) for Q2DEG with one filled subband, vs the in-plane momentum, shown for three values of the density parameter r_s. EXX and LDA-based quantities are plotted with solid and dashed lines, respectively. The minus KS eigenvalues $-\epsilon_0$ are shown with horizontal straight lines.

Our expansion of DM in λ may not necessarily be based on TDEXX, but we could have used other TDDFT schemes as well. Then the resulting series could, likewise, be expected to converge to the physical DM. In Fig. 2 we, therefore, compare EXX results to those of the local density approximation (LDA) (dashed lines). An eloquent conclusion is that, while the KS eigenvalues, being auxiliary quantities, are completely different in the respective approximations (horizontal lines), the IPs we obtain, being approximations to observables, are found close to each other in EXX and LDA. Obviously, the latter is of great practical consequence, since it shows that inexpensive local functionals can be successfully used in the framework of this theory.

In Fig. 3, we plot the interacting electrons' emission intensity and compare it with its Fermi's golden rule counterpart. It must be noted that the golden rule is overwhelmingly often used in the literature with the KS field in the matrix element replaced with the bare external one (dipole approximation), while the screening has been included only rather recently [24]. It is, therefore, instructive to compare our results to the both variants of the conventional formula. Without interaction, the threshold of

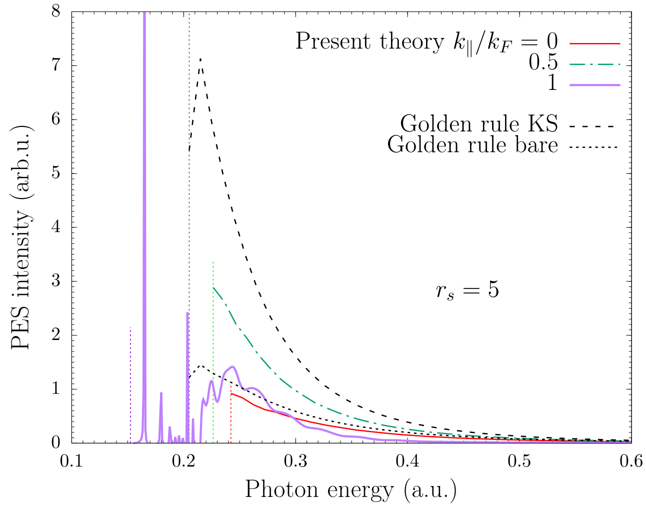

FIG. 3. Spectra of photoemission from the Q2DEG with one subband filled. Results of our theory [sum of Eqs. (18) and (20)] are shown with the thin solid red, dashed-dotted green, and thick solid purple lines, for $k_\parallel/k_F = 0, 0.5$, and 1, respectively. Results for Fermi's golden rule using the KS potential $v_s^{(1)}$ [Eq. (18)], and with the bare external potential $v_{\rm ext}^{(1)}$, are shown with dashed and dotted lines, respectively. The threshold of photoemission is indicated in each case by a short vertical dotted straight line.

the photoemission lies at $-\epsilon_0$, shown in Fig. 3 with a long vertical dotted line, and it is the same for all values of $k_\parallel$. As discussed above, this is not the case with the interaction included, and the corresponding thresholds $\omega_{\rm th}(k_\parallel) = -\epsilon_0 - \Delta\omega(k_\parallel)$ for three values of $k_\parallel$ are shown by short vertical dotted lines. The spectra at different $k_\parallel$ are very different from each other, signifying the important quantitative role of the interaction effect. The case of $k_\parallel = k_F$ deserves special attention: Here $\Delta\omega > 0$, which makes emission possible at $\omega < -\epsilon_0$. In this regime, the spectrum is strongly affected by the transitions to the discreet excited states, resulting in resonances at the corresponding energies. Since within TDEXX these transitions are undamped [21], the amplitudes of the corresponding peaks are not in the same scale with the rest of the spectra.

Isolated atoms.—Our second example concerns photoemission from atoms. In Table I we list the KS EXX eigenvalues, the energy shifts, and the total IP according to the present theory. The following important observations can be made. First, for the highest energy levels, the shifts $\Delta\omega$ disappear, which is in agreement with the IP theorem. Second, for inner levels, $\Delta\omega$ are large and they change the KS eigenvalues in the right direction to the experimental IP. These shifts are, however, too big, making the theoretical IP to overestimate the experimental ones, while the KS values underestimate them. Obviously, further terms in the series in λ are necessary to improve the agreement with experiment. Third, our $\epsilon_i + \Delta\omega_i$ are found very close to the HF eigenvalues. This has a fundamental reason: As follows from the discussion after Eq. (13), the latter give physical IP to the first order in the interaction, which also $\epsilon_i + \Delta\omega_i$ do, but not ϵ_i.

As seen from Table II, similarly to the case of Q2DEG, the use of LDA instead of EXX does not change the IP significantly: while the orbital eigenvalues differ largely in the corresponding approximations, adding $\Delta\omega$ brings them close together.

TABLE I. KS EXX orbital eigenvalues ϵ_i, the energy shifts $\Delta\omega_i$ of Eq. (24), and the corresponding interaction-corrected IP $-(\epsilon_i + \Delta\omega_i)$ for several spherically symmetric spin neutral atoms, compared to the experimental [25] and the HF [26] values.

Atom	$-\epsilon_i$	$-\Delta\omega_i$	$-(\epsilon_i + \Delta\omega_i)$	$-\epsilon_i^{\rm exp}$	$-\epsilon_i^{\rm HF}$
He(1s)	0.9179	-9.6×10^{-14}	0.9179	0.9036	0.9179
Be(1s)	4.1147	0.6169	4.7316	4.384	4.7327
(2s)	0.3091	-2.7×10^{-6}	0.3091	0.3425	0.3093
Ne(1s)	30.767	1.9951	32.762	31.985	32.772
(2s)	1.7054	0.2187	1.9241	1.781	1.9304
(2p)	0.8478	-5.4×10^{-5}	0.8477	0.7960	0.8504
Mg(1s)	46.267	2.7567	49.024	48.174	49.032
(2s)	3.0927	0.6697	3.7624	3.454	3.7677
(2p)	1.8696	0.4114	2.2811	2.0212	2.2822
(3s)	0.2526	3.2×10^{-5}	0.2526	0.2811	0.2531

In conclusion, assuming a solution to the TDDFT problem for a quantum mechanical system known, we have evaluated the reduced density matrix $\rho(\mathbf{r}, \mathbf{r}', t)$ to the first order in the $e-e$ interaction, at the fixed particle density, as stipulated by TDDFT. The knowledge of $\rho(\mathbf{r}, \mathbf{r}', t)$ extends the theory to phenomena, which are beyond the reach of the pure TDDFT with presently existing observable functionals. As a particular application, we have derived an extension to Fermi's golden rule for the momentum-resolved stationary photoelectron spectroscopy, which accounts for the interparticle interaction.

Our calculations for the quasi-2D electron gas with one filled subband and for isolated atoms manifest an important role of the *e*-*e* interactions in the TDDFT of PES. In particular, our theory captures a remarkable effect of the correlation between the in-plane and the normal motion in a laterally uniform system, which is a feature due to the many-body interactions.

Going beyond the bare exchange remains the main challenge in the future development of the theory. Although, on the formal level, our method contains all the correlations at λ^n, $n \geq 2$, at present only the inclusion of the λ^2 term looks feasible. Since this method involves the TDDFT calculation followed by the construction of the reduced DM, it comes very encouraging that, as both our examples show, the inaccuracies of the former are compensated by the latter. This opens the way to use the inexpensive local TDDFT functionals without compromising the accuracy of the final results, which greatly contributes to the practicability of this method.

Among other extensions of the theory, we note that the nonlinear dynamics using Eq. (15) provides a natural pathway to the quantum-mechanically consistent inclusion of interactions in the theory of photoemission in the time domain [27–32]; presently this theory relies on the ansatz of the identification of the KS particles with physical electrons [30]. Finally, we anticipate it conceptually feasible to extend the theory to evaluate the two-electron density matrix, with an immediate application to the double photoelectron spectroscopy.

TABLE II. KS LDA and EXX orbital eigenvalues and the corresponding interaction-corrected IP of the atoms in Table I.

Atom	$-\epsilon_i^{\rm LDA}$	$-\epsilon_i^{\rm EXX}$	$-(\epsilon_i^{\rm LDA} + \Delta\omega_i^{\rm LDA})$	$-(\epsilon_i^{\rm EXX} + \Delta\omega_i^{\rm EXX})$
He(1s)	0.5170	0.9179	0.9354	0.9179
Be(1s)	3.7956	4.1147	4.7547	4.7316
(2s)	0.1736	0.3091	0.3123	0.3091
Ne(1s)	30.229	30.767	32.849	32.762
(2s)	1.2656	1.7054	1.9741	1.9241
(2p)	0.4428	0.8478	0.8958	0.8477
Mg(1s)	45.890	46.267	49.090	49.024
(2s)	2.8454	3.0927	3.7874	3.7624
(2p)	1.6615	1.8696	2.3102	2.2811
(3s)	0.1423	0.2526	0.2542	0.2526

V. U. N. acknowledges support from the Ministry of Science and Technology, Taiwan, Grants No. 106–2923–M-001–002–MY3 and No. 107–2112–M–001–033.

---

[*] nazarov@gate.sinica.edu.tw

[1] A. Zangwill and P. Soven, Density-functional approach to local-field effects in finite systems: Photoabsorption in the rare gases, Phys. Rev. A **21**, 1561 (1980).

[2] E. Runge and E. K. U. Gross, Density-Functional Theory for Time-Dependent Systems, Phys. Rev. Lett. **52**, 997 (1984).

[3] E. K. U. Gross and W. Kohn, Local Density-Functional Theory of Frequency-Dependent Linear Response, Phys. Rev. Lett. **55**, 2850 (1985).

[4] Y.-H. Kim and A. Görling, Exact Kohn-Sham exchange kernel for insulators and its long-wavelength behavior, Phys. Rev. B **66**, 035114 (2002).

[5] S. Botti, F. Sottile, N. Vast, V. Olevano, L. Reining, H.-C. Weissker, A. Rubio, G. Onida, R. Del Sole, and R. W. Godby, Long-range contribution to the exchange-correlation kernel of time-dependent density functional theory, Phys. Rev. B **69**, 155112 (2004).

[6] P. M. Echenique, R. M. Nieminen, and R. Ritchie, Density functional calculation of stopping power of an electron gas for slow ions, Solid State Commun. **37**, 779 (1981).

[7] V. U. Nazarov, J. M. Pitarke, C. S. Kim, and Y. Takada, Time-dependent density-functional theory for the stopping power of an interacting electron gas for slow ions, Phys. Rev. B **71**, 121106(R) (2005).

[8] V. U. Nazarov, G. Vignale, and Y.-C. Chang, Dynamical many-body corrections to the residual resistivity of metals, Phys. Rev. B **89**, 241108(R) (2014).

[9] L. D. Landau and E. M. Lifshitz, *Quantum Mechanics: The Non-Relativistic Theory* (Butterworth-Heinemann, London, 1981).

[10] According to the general principles of TDDFT, all physical quantities, including the momentum distribution, are determined by the particle density. The corresponding observable functionals are not, however, known, which necessitates such studies as ours.

[11] A. Görling and M. Levy, Exact Kohn-Sham scheme based on perturbation theory, Phys. Rev. A **50**, 196 (1994).

[12] A. Görling, Time-dependent Kohn-Sham formalism, Phys. Rev. A **55**, 2630 (1997).

[13] W. Kohn and L. J. Sham, Self-consistent equations including exchange and correlation effects, Phys. Rev. **140**, A1133 (1965).

[14] M. E. Casida, Time-dependent density functional response theory for molecules, in *Recent Advances in Density Functional Methods* (World Scientific, Singapore, 1995), pp. 155–192.

[15] See Supplemental Material at http://link.aps.org/supplemental/10.1103/PhysRevLett.123.095302 for the derivation of (I) Eqs. (9)–(10), (II) Eqs. (17)–(18), (III) Eqs. (19)–(22), and (IV) for the reduction of the theory in the case of the Q2DEG with one filled subband.

[16] R. T. Sharp and G. K. Horton, A variational approach to the unipotential many-electron problem, Phys. Rev. **90**, 317 (1953).

[17] J. D. Talman and W. F. Shadwick, Optimized effective atomic central potential, Phys. Rev. A **14**, 36 (1976).

[18] C. A. Ullrich, U. J. Gossmann, and E. K. U. Gross, Time-Dependent Optimized Effective Potential, Phys. Rev. Lett. **74**, 872 (1995).

[19] C. Møller and M. S. Plesset, Note on an approximation treatment for many-electron systems, Phys. Rev. **46**, 618 (1934).

[20] The contribution from the $\rho^{(1)}$ term is zero identically.

[21] V. U. Nazarov, Quasi-Low-Dimensional Electron Gas With One Populated Band as a Testing Ground for Time-Dependent Density-Functional Theory of Mesoscopic Systems, Phys. Rev. Lett. **118**, 236802 (2017).

[22] J. P. Perdew, R. G. Parr, M. Levy, and J. L. Balduz, Density-Functional Theory for Fractional Particle Number: Derivative Discontinuities of the Energy, Phys. Rev. Lett. **49**, 1691 (1982).

[23] Interestingly, the IP-theorem holds, in this case, “on average,” i.e., IP $(k_\parallel)$, averaged over $\mathbf{k}_\parallel$, equals the minus KS eigenvalue, since $\int_{k_\parallel \le k_F} \Delta\omega(k_\parallel) d\mathbf{k}_\parallel = 0$, as can be verified by Eqs. (26)–(28) and (25).

[24] E. E. Krasovskii, V. M. Silkin, V. U. Nazarov, P. M. Echenique, and E. V. Chulkov, Dielectric screening and band-structure effects in low-energy photoemission, Phys. Rev. B **82**, 125102 (2010).

[25] D. A. Shirley, R. L. Martin, S. P. Kowalczyk, F. R. McFeely, and L. Ley, Core-electron binding energies of the first thirty elements, Phys. Rev. B **15**, 544 (1977).

[26] S. L. Saito, Hartree-Fock-Roothaan energies and expectation values for the neutral atoms He to Uuo: The B-spline expansion method, At. Data Nucl. Data Tables **95**, 836 (2009).

[27] A. Pohl, P.-G. Reinhard, and E. Suraud, Towards Single-Particle Spectroscopy of Small Metal Clusters, Phys. Rev. Lett. **84**, 5090 (2000).

[28] U. De Giovannini, D. Varsano, M. A. L. Marques, H. Appel, E. K. U. Gross, and A. Rubio, *Ab initio* angle- and energy-resolved photoelectron spectroscopy with time-dependent density-functional theory, Phys. Rev. A **85**, 062515 (2012).

[29] P. M. Dinh, P. Romaniello, P.-G. Reinhard, and E. Suraud, Calculation of photoelectron spectra: A mean-field-based scheme, Phys. Rev. A **87**, 032514 (2013).

[30] M. Dauth and S. Kümmel, Predicting photoemission intensities and angular distributions with real-time density-functional theory, Phys. Rev. A **93**, 022502 (2016).

[31] P. Wopperer, U. De Giovannini, and A. Rubio, Efficient and accurate modeling of electron photoemission in nanostructures with TDDFT, Eur. Phys. J. B **90**, 51 (2017).

[32] U. De Giovannini, H. Hübener, and A. Rubio, A first-principles time-dependent density functional theory framework for spin and time-resolved angular-resolved photoelectron spectroscopy in periodic systems, J. Chem. Theory Comput. **13**, 265 (2017).